2009 American Control Conference
Hyatt Regency Riverfront, St. Louis, MO, USA
June 10-12, 2009

A New Robust Damping and Tracking Controller for SPM Positioning Stages

Andrew J. Fleming, Sumeet S. Aphale and S. O. Reza Moheimani

Abstract— **This paper demonstrates a simple second-order controller that eliminates scan-induced oscillation and provides integral tracking action. The controller can be retrofitted to any scanning probe microscope with position sensors by implementing a simple digital controller or op-amp circuit. The controller is demonstrated to improve the tracking bandwidth of an NT-MDT scanning probe microscope from 15 Hz (with an integral controller) to 490 Hz while simultaneously improving gain-margin from 2 dB to 7 dB. The penalty on sensor induced positioning noise is minimal.**

For the Scanning Probe Microscope considered in this paper, the noise is marginally increased from 0.30 nm RMS to 0.39 nm RMS. Open- and closed-loop experimental images of a calibration standard are reported at speeds of 1 and 10 lines per second (with a scanner resonance frequency of 290 Hz). Compared to traditional integral or PID controllers, the proposed controller provides a bandwidth improvement of approximately ten times. This allows faster imaging and less tracking lag at low speeds.

I. Introduction

To investigate matter at nanometer and sub-nanometer scales, scanning probe microscopy was introduced more than two decades ago [1], [2]. A key component of these instruments is the nanopositioning stage used to scan or position the probe or sample. Many nanopositioning device geometries have been proposed and tested for this purpose [3], [4], [5], [6]. However, due to the simplicity of manufacture and the large size-to-motion ratio, piezoelectric tube scanners have become the most popular devices used in commercial SPM systems [7].

These tube scanners have two inherent problems that degrade the positioning performance of the scanner, viz: (i) Resonant modes due to the mechanical construction [8] and (ii) Nonlinear behavior due to hysteresis and creep in the piezoelectric material [9].

Piezoelectric tube scanners feature a dominant, lightly damped, low-frequency resonant mode in their frequency response. High-frequency components of the reference input and/or exogenous noise can excite this resonant mode causing erroneous vibration and large positioning errors. In most piezoelectric tubes applications, the fastest possible open-loop scan frequency is limited to less than 1% of the resonance frequency. Though the frequency of this resonant mode depends on the physical dimensions of the tube scanner, typical resonance frequencies are less than 1 kHz. Thus, the fastest achievable scans are at speeds of less than 10 Hz. This speed constraint is further restricted by the presence of piezoelectric nonlinear effects such as hysteresis and creep. These nonlinearities necessiate the use of closed-loop tracking controllers such as integral controllers. Detrimentally, controllers with integral action are severely limited in bandwidth by the mechanical resonance which imposes a low gain-margin. Contrary to the low speed achievable with piezoelectric tube scanners, many scanning applications are demanding faster scan rates with greater accuracy and resolution, [10], [11], [12], [13], [14].

To reduce errors resulting from the system resonance, various closed-loop damping techniques have been proposed. Positive position feedback control and polynomial based controller designs have been shown to adequately damp the resonant mode, see [15] and [16]. The application of active and passive shunt damping techniques for piezoelectric tube scanners was reported in [17] and [18]. Other active damping techniques, such as resonant control, have also been proposed, see [19], [20]. For a detailed overview on this topic, the reader is referred to [21]. Recently, the Integral Resonant Control (IRC) scheme was demonstrated as a simple means for damping multiple resonance modes of a cantilever beam [22]. The IRC scheme employs a constant feedthrough term and a simple integrator-based first-order controller to achieve substantial damping of multiple resonance modes. In [23], IRC was shown to have a favorable output-to-disturbance response and is thus ideal for nanopositioning applications. Also, a simple tracking controller was combined with the IRC damping technique to deliver accurate tracking performance. Due to its implementation simplicity and the improvement in tracking bandwidth, the IRC damping scheme with integral action is an excellent alternative to standard proportional-integral (PI) control algorithms used in commercial SPMs.

A. Contribution of this work

In this work, we demonstrate an IRC damping controller with integral tracking action applied to an NT-MDT Ntegra scanning probe microscope. Experimental results show greater than ten times improvement in tracking bandwidth with improved stability margins and disturbance rejection. This allows the microscope to operate at speeds exceeding 30 lines per second with no mechanical modifications.

This paper is organized as follows. Section II describes the experimental setup. Details of the control design are then given in Section III. The controller is then implemented in Section IV. Open- and closed-loop scan results are also compared in this section. The noise performance is evaluated in Section V followed by conclusions in Section VI.

II. Experimental Setup

An NT-MDT Ntegra SPM was used to implement and test the proposed control strategy. A signal access module allows direct access to the scanner electrodes and reference trajectory. The scanner is an NT-MDT Z50309cl piezoelectric tube scanner with 100 μm range. The tube scanner has quartered internal and external electrodes allowing the scanner to be driven in a bridged configuration. That is, the internal and external electrodes are driven with equal but opposite voltages. Capacitive sensors are used to measure the resulting displacement in each axis with a sensitivity of 0.158 Volts per micrometer.

For modeling purposes, the scanner is treated as a two-input two-output system. The two inputs are the voltages applied to the x- and y-axis amplifiers while the outputs are the corresponding capacitive sensor voltages. All of the frequency responses were recorded with an HP-35670A

This work was supported by the Australian Research Council (DP0666620) and the Center of Excellence for Complex Dynamic Systems and Control

Andrew J. Fleming andrew.fleming@newcastle.edu.au and S. O. Reza Moheimani are with the School of Electrical Engineering and Computer Science at the University of Newcastle, Callaghan, NSW, Australia

Sumeet S. Aphale is a Research Fellow at the Center for Applied Dynamics Research (CADR), School of Engineering, Kings College, University of Aberdeen, Aberdeen, UK

(a)

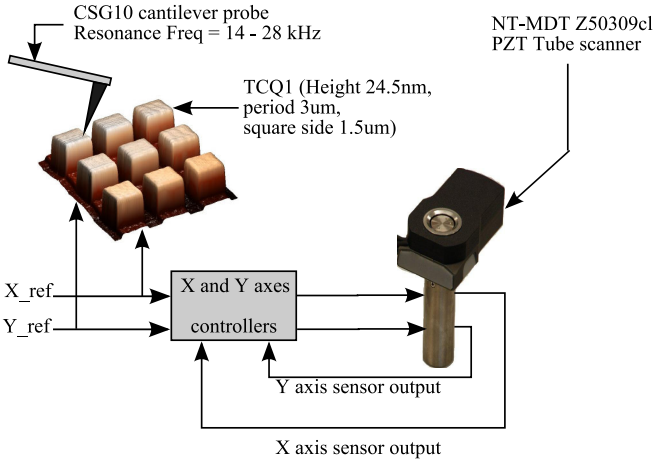

(b)

Fig. 1. (a) NT-MDT Ntegra scanning probe microscope. (b) Experimental scanner configuration.

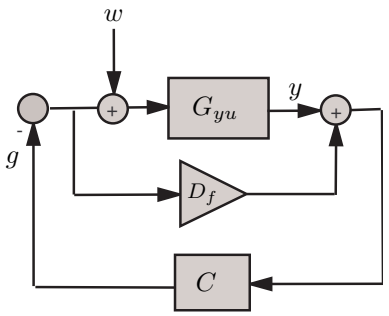

Fig. 2. Integral resonant control scheme [22]

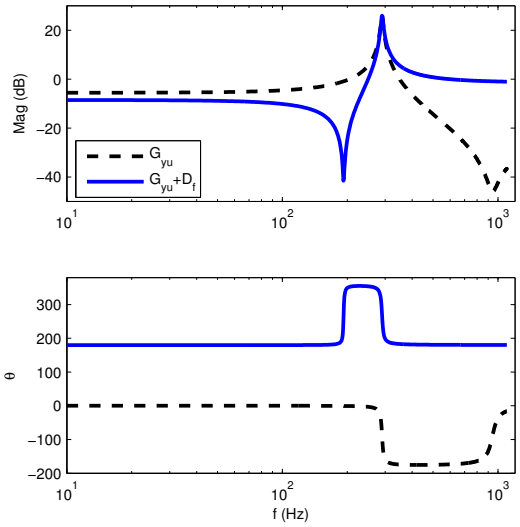

Fig. 3. Frequency response from the applied x-axis voltage to the measured sensor voltage in the same axis G_{yu}. The system with artificial feedthrough is also shown $G_{yu} + D_f$, where D_f = -0.9.

Spectrum Analyzer. The control strategy was implemented using a dSPACE-1103 rapid prototyping system.

III. Control Design

The foremost control objective in nanopositioning is to minimize tracking error. As the system is non-linear, this requires integral action in the control loop. For high-speed operation the closed-loop system must be inverted either offline or with a feedforward controller. Although this is straight-forward to accomplish, the resulting performance can be highly sensitive to small changes in resonance frequency. In this work, a damping controller is utilized to attenuate the system's first resonant mode. This provides improved bandwidth without the need for accurate plant models or inversion. The damping controller is highly robust to changes in resonance frequency and also provides improved disturbance rejection.

A. Damping Controller

As discussed in the introduction, IRC was introduced as a means for augmenting the structural damping of resonant systems with collocated sensors and actuators. A diagram of an IRC loop is shown in Figure 2. It consists of the collocated system G_{yu}, an artificial feedthrough D_f and a controller C. The input disturbance w represents both environmental disturbance and non-linearity due to piezoelectric hysteresis.

The first step in IRC design is to select the feedthrough term D_f. The combination of G_{yu} and D_f can then be considered a new system $G_{yu} + D_f$. By choosing D_f sufficiently large and negative, the system $G_{yu}+D_f$ contains a pair of zeros below the frequency of the first resonant mode [18]. The frequency responses of the open-loop system G_{yu} and the modified transfer function $G_{yu} + D_f$ are plotted in Figure 3.

A key observation is that the phase of $G_{yu} + D_f$ lies between 0 and -180 degrees. Thus, a negative integral controller

$$C = \frac{-k}{s}, \tag{1}$$

adds a constant phase lead of 90 degrees to the loop-gain. The phase response of the resulting loop-gain now lies between +90 and -90 degrees. That is, regardless of controller gain, the closed-loop system has a phase margin of 90 degrees.

A suitable controller gain k can easily be selected to maximize damping using the root-locus technique [18].

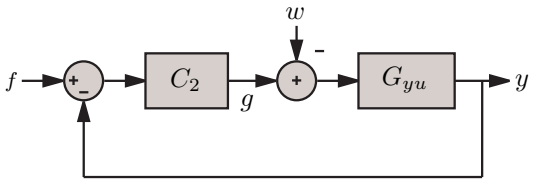

Fig. 4. The integral resonant controller of Figure 2 rearranged in regulator form

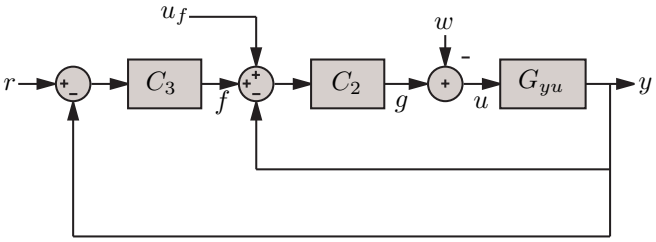

Fig. 5. Tracking control system with the damping controller $C_2(s)$ and tracking controller $C_3(s)$. The feedforward input u_f is discussed in Section III-C.

B. Tracking Controller

After implementing an IRC controller, shown in Figure 2, a secondary integral control loop cannot be directly closed around the output of G_{yu}. The feedthrough term D_f and the location of the summing junction prevent the possibility for integral action.

To incorporate an additional control loop, the feedback diagram must be rearranged so that an additional input does not appear as a disturbance. This can be achieved by finding an equivalent regulator that provides the same loop gain but with an input suitable for tracking control. In Figure 2, the control input g is related to the measured output y by

$$g = C(y - gD_f), \tag{2}$$

thus, the equivalent regulator C_2 is

$$C_2 = \frac{C}{1 + CD_f}. \tag{3}$$

When $C = \frac{-k}{s}$ the equivalent regulator is

$$C_2 = \frac{-k}{s - kD_f}. \tag{4}$$

A diagram of the equivalent regulator loop formed by C_2 and G is shown in Figure 4. This loop is easily enclosed in a secondary outer loop to achieve integral tracking. A control diagram of this configuration is shown in Figure 5. Due to the inverting behavior of the IRC loop, the tracking controller C_3 is a negative integral controller

$$C_3 = \frac{-k_i}{s}. \tag{5}$$

The transfer function of the closed-loop system is

$$\frac{y}{r} = \frac{C_2 C_3 G_{yu}}{1 + C_2(1 + C_3)G_{yu}}, \tag{6}$$

In addition to the closed-loop response, the transfer function from disturbance to the regulated variable y is also of importance. This can be found as

$$\frac{y}{w} = \frac{G_{yu}}{1 + C_2(1 + C_3)G_{yu}}. \tag{7}$$

Controller	C_3	C_2	u_f	Bandwidth
Integral (I)	$\frac{(80)}{s}$	0	0	15 Hz
I + FF	$\frac{(80)}{s}$	0	1.88	251 Hz
I + IRC + FF	$\frac{-(400)}{s}$	$\frac{-(1800)}{s-(1800)(-0.9)}$	0.91	490 Hz

TABLE I
SUMMARY OF IMPLEMENTED CONTROLLERS AND RESULTING CLOSED-LOOP BANDWIDTH

That is, the disturbance input is regulated by the equivalent controller $C_2(1 + C_3)$.

C. Feedforward input

Feedforward inputs can be used to improve the bandwidth of a closed-loop system by bypassing the tracking controller or inverting dynamics [24], [25], [26]. Inversion based feedforward provides the best performance but is also sensitive to modeling inaccuracies and system variations during service. Here, where a change in resonance frequency from 260 to 900 Hz is considered, inversion based feedforward cannot be applied. Such wide variations in resonance frequency would result in unacceptable modeling error and detrimental feedforward performance [27]. However, simply using the inverse DC gain of the system provides some improvement in tracking lag and is beneficial in this application.

In Figure 5, the feedforward input is denoted u_f. This signal is generated from the reference input and the DC gain of the damped system, that is,

$$u_f = r \left(\frac{C_2 G_{yu}}{1 + C_2 G_{yu}} \bigg|_{s=0} \right)^{-1}. \tag{8}$$

IV. EXPERIMENTAL IMPLEMENTATION

A. Controller design

In this section, the proposed control scheme is implemented on the AFM discussed in Section IV. For the sake of comparison, three controllers were considered: 1) an integral tracking controller; 2) an integral tracking controller with feedforward; and 3) an integral tracking controller with IRC damping and a feedforward input. Diagrams of the three control strategies are pictured in Figure 6. The design and performance of each controller is discussed below. A summary of the controllers is contained in Table I.

1) Integral tracking controller: The integral tracking controller was designed to maximize tracking bandwidth. The maximum gain was restricted to k_i=80 by the gain-margin of only 2.5 dB. The low gain-margin is due to the lightly damped resonance mode at 575 Hz. As the resonance has a sharp phase response at a frequency much higher than the controller's crossover frequency, the system phase margin is dominated by the integral controller and remains at 90 degrees. The experimental frequency response, showing a 15 Hz bandwidth, and time domain response to a 10 Hz triangular scan is shown in Figure 6.

2) Integral controller with feedforward: By adding a feedforward input to the integral controller, as shown in Figure 6, the bandwidth can be extended to 251 Hz. However, the majority of this bandwidth is uncontrolled and the open-loop dynamics now appear in the tracking response. The time domain response exhibits significant oscillation which is highly undesirable in microscopy applications.

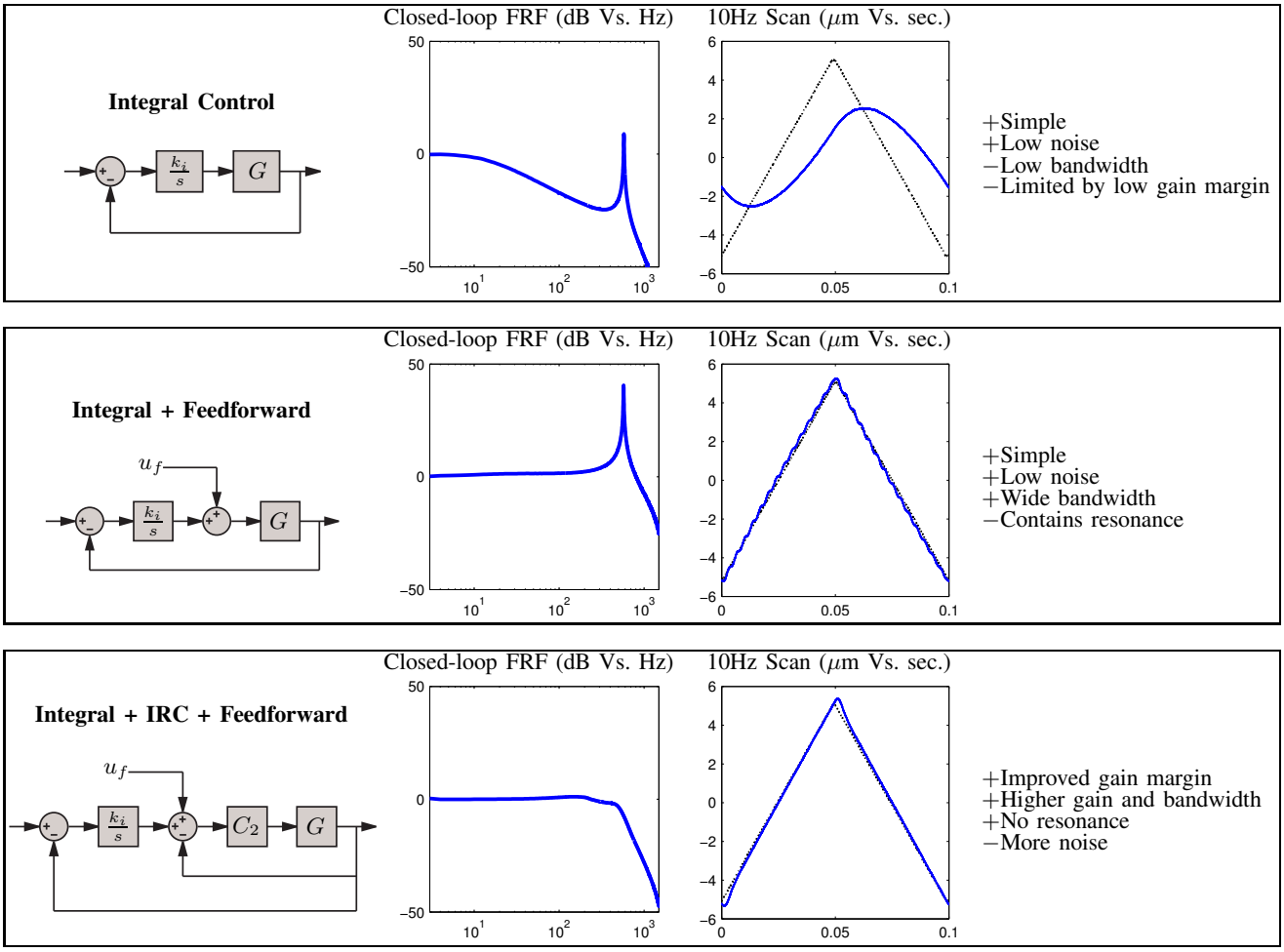

Fig. 6. Comparison of control strategies from simplest to more complicated. The frequency responses are measured from the applied reference to the measured sensor voltage.

3) Integral controller with IRC damping and feedforward: Following the procedure in Section III-B an IRC damping controller was first designed for the system. From a root-locus plot, the maximum damping was found to occur at k=1800. An integral controller was then designed for the damped system. With a gain of k_i=400 the resulting closed-loop system has a bandwidth of 490 Hz while maintaining a 7 dB gain-margin and 50 degree phase-margin. This is a vast improvement in both bandwidth and stability margins compared to the controller in Section IV-A.1.

B. Imaging performance

In this section, experimental images are presented that demonstrate the imaging consequences of scanner oscillations and the improvements that can be achieved with resonance control.

The sample under consideration is a MikroMasch TCQ1 grating with a feature height of 24.5 nm and period of 3 um. Pictured in Figure 7, this grating is useful for quantifying oscillation and non-linearity in both axes simultaneously. All of the following images were recorded in constant-height contact mode with a NT-MDT CSG10 cantilever with a resonance frequency of 20 kHz and stiffness of 0.1 N/m.

Images of the grating were recorded in open- and closed-loop at 1 and 10-Hz line rates. At 1 Hz, there is no distinguishable difference between open- and closed-loop control and these images are not included. In Figure 8, the oscillation in the open-loop 10 Hz scan is clearly visible in both the image and measured x-axis displacement. With the controller activated, the oscillation and corresponding artifacts are eliminated.

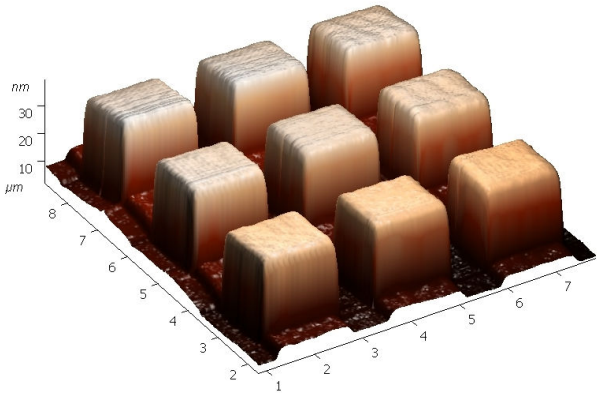

Fig. 7. MikroMasch TGQ1 calibration grating. The feature height is 24.5 nm with 3 μm period. This image was obtained using constant-force contact mode with a 1 Hz line rate and image was

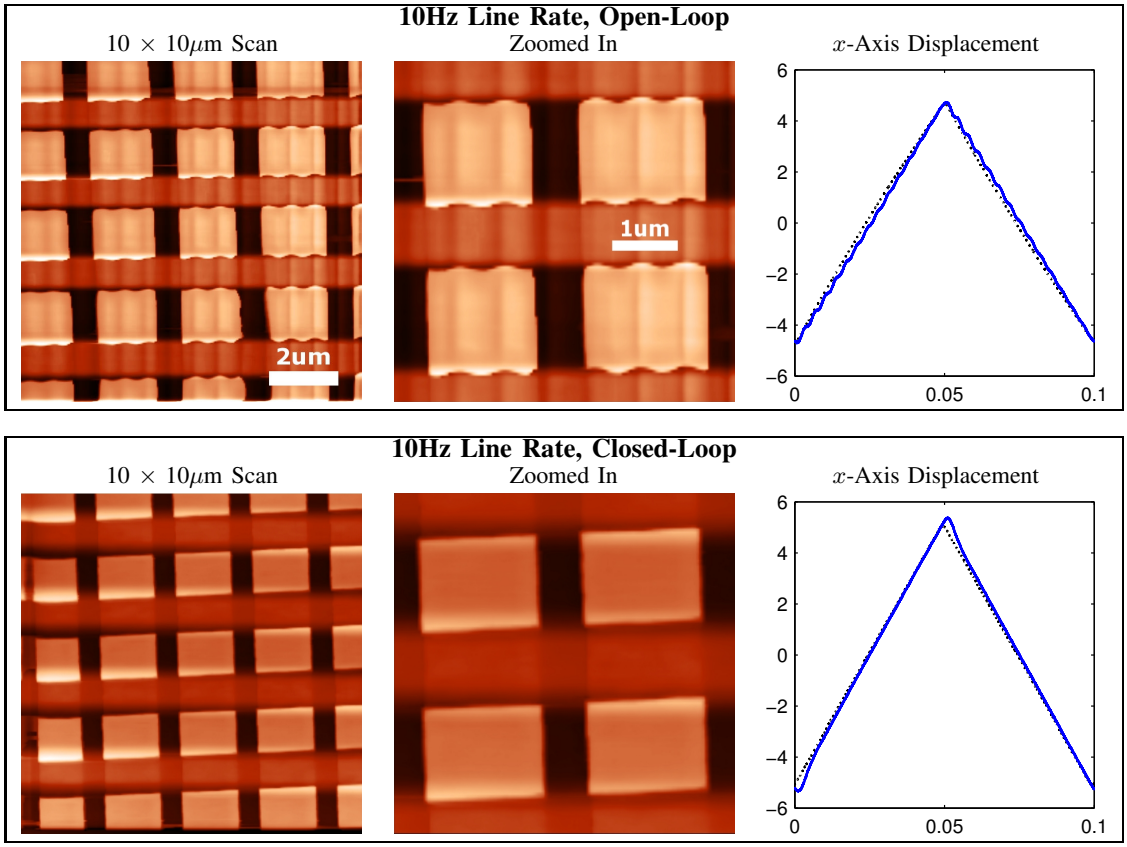

Fig. 8. A comparison of images recorded at 10 Hz with open- and closed-loop control of the sample scanner

At higher scan rates where overshoot and tracking lag become significant, the performance can be improved by model based inversion [26] but at the expense of robustness [27]. As this work aims to provide good performance over an extremely wide range of operating conditions, feedforward inversion is not considered beneficial. Performance improvements can also be achieved by shaping the input triangle signal to remove energy above the fifth harmonic. A review of techniques for achieving this and a method for generating optimal input signals is contained in reference [28]. These techniques are not used here as they require modification of the microscope control logic and are thus not immediately straight-forward to implement, which is a requisite in this paper.

C. Performance robustness

During service, the sample mass and resonance frequency of SPM scanners can vary widely. The highest resonance frequency occurs while the scanner is unloaded, this can drop by 80% as additional mass such as liquid cells and heating elements are added. Such large variations in resonance frequency are not often discussed in the literature as it can be extremely difficult to design controllers that are even stable, let alone provide reasonable performance, over such ranges. However, to be of practical value to SPM users and designers, this issue is of primary concern.

One of benefits of the control technique discussed in Section III-A is that it is highly robust to changes in resonance frequency with respect to both stability and performance. This is a unique characteristic which is ideal for SPM scanner control. For the microscope described in Section II, the resonance frequency is 934 Hz when unloaded. With a sample holder and heating element, this reduces to 290 Hz.

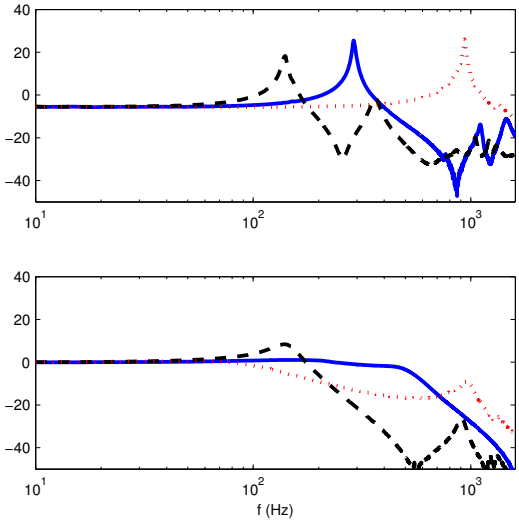

Fig. 9. The open-loop (top) and closed-loop (bottom) magnitude frequency response from the reference input voltage r to measured sensor voltage y (in dB). The three curves demonstrate the greatest range in frequency response that could occur in practice. The resonance frequencies range from the fully loaded case of 140 Hz (dashed line), to the nominal resonance frequency of 290 Hz (solid line), to the unloaded frequency of 934 Hz (dotted line).

A further reduction to 140 Hz is possible if additional mass such as a liquid cell or magnetic coil is added. The open-loop frequency response under these conditions is plotted in Figure 9. Also shown is the closed-loop response. In all cases, the controller remains stable and provides good per-

formance that decays gracefully as the resonance frequency drops. The main limitation to robustness is the integral tracking controller C_3. With decreasing resonance frequency, the phase margin of this controller slowly degrades, hence, it must be designed to tolerate the lowest expected resonance frequency. As the phase margin reduces, there is also some peaking introduced into the closed-loop tracking response, this can be observed for the lowest resonance frequency in Figure 9.

V. Noise Penalty

To quantify the practical impact on positioning performance, both the noise sensitivity and noise density must be taken into account. By measuring the actual sensor noise, its effect on positioning noise can be simulated by filtering with the noise sensitivity. Using a three second record of the sensor noise, the RMS positioning noise was found to be 0.30 nm for the basic integral controller and 0.39 nm for the IRC controller. Considering that the closed-loop bandwidth has been increased from 15 to 490 Hz, the increase in RMS noise from 0.30 to 0.39 nm is negligible.

VI. Conclusions

In this paper, Integral Resonant Control (IRC) was applied to damp the first resonant mode of a scanning probe microscope positioning stage. Compared to a standard integral tracking controller, the IRC controller permitted an increase in closed-loop tracking bandwidth from 15 to 490 Hz. The stability margins were simultaneously improved from 2.5 dB to 7 dB gain margin. Although the higher performance controller has a wider noise bandwidth, this bandwidth does not include the lightly damped resonance exhibited by standard tracking controllers. Consequently, the positioning noise was only increased from 0.30 nm to 0.39 nm RMS. This is a negligible increase considering the large improvements in tracking bandwidth and image quality.

Aside from the improved performance, other benefits of the proposed controller include ease of implementation and robustness. As the combined IRC and tracking controller is only second order, it is easily implemented with a simple analog circuit. The controller is also extremely robust to changes in resonance frequency.

Closed-loop stability and satisfactory performance was achieved in spite of a resonance frequency variation from 290 Hz to 934 Hz. Such large variations are commonly exhibited by piezoelectric tube scanners used with small samples and larger loads, for example, liquid cells and heating stages.

Experimental images using an NT-MDT microscope demonstrated substantial improvement in image quality due to the elimination of scan-induced vibration.

References

[1] G. Binnig and H. Rohrer, "The scanning tunneling microscope," *Scientific American*, vol. 253, pp. 50–56, 1986.

[2] S. M. Salapaka and M. V. Salapaka, "Scanning probe microscopy," *IEEE Control Systems Magazine*, vol. 28, no. 2, pp. 65–83, April 2008.

[3] R. Koops and G. A. Sawatzky, "New scanning device for scanning tunneling microscope applications," *Review of Scientific Instruments*, vol. 63, no. 8, pp. 4008–4009, Aug 1992.

[4] T. Ando, N. Kodera, D. Maruyama, E. Takai, K. Saito, and A. Toda, "A high-speed atomic force microscope for studying biological macromolecules in action," *Japanese Journal of Applied Physics*, vol. 41, no. 7B, pp. 4851–4856, 2002.

[5] A. Sebastian and S. M. Salapaka, "Design methodologies for robust nano-positioning," *IEEE Trans. on Control Systems Technology*, vol. 13, no. 6, pp. 868–876, November 2005.

[6] G. Schitter, K. J. Åstrom, B. DeMartini, P. J. Thurner, K. L. Turner, and P. K. Hansma, "Design and modeling of a high-speed AFM-scanner," *IEEE Trans. on Control Systems Technology*, vol. 15, no. 5, pp. 906–915, 2007.

[7] S. O. R. Moheimani, "Invited review article: Accurate and fast nanopositioning with piezoelectric tube scanners: Emerging trends and future challenges," *Review of Scientific Instruments*, vol. 79, no. 7, pp. 071 101–1–071 101–11, July 2008.

[8] G. Schitter and A. Stemmer, "Identification and open-loop tracking control of a piezoelectric tube scanner for high-speed scanning probe microscopy," *IEEE Trans. on Control Systems Technology*, vol. 12, no. 3, pp. 449–454, 2004.

[9] *Piezoelectric Ceramics: Principles and Applications*. APC International Ltd., 2006.

[10] B. Yao, F.-S. Chien, S. Chen, P.-W. Lui, and G. Peng, "Scanning probe lithography with real time position control interferometer," *Proceedings of the IEEE-NANO Conference*, pp. 13–15, 2002.

[11] G. Yang, J. A. Gaines, and B. J. Nelson, "A supervisory wafer-level 3D microassembly system for hybrid MEMS fabrication," *Journal of Intelligent and Robotic Systems*, vol. 37, no. 1, pp. 42–68, 2003.

[12] M. J. Rost, L. Crama, P. Schakel, E. van Tol, G. B. E. M. van Velzen-Williams, C. F. Overgauw, H. ter Horst, H. Dekker, B. Okhuijsen, M. Seynen, A. Vijftigschild, P. Han, A. J. Katan, K. Schoots, R. Schumm, W. van Loo, T. H. Oosterkamp, and J. W. M. Frenken, "Scanning probe microscopes go video rate and beyond," *Review of Scientific Instruments*, vol. 76, pp. 053 710–1–053 710–9), 2005.

[13] S. Thian, Y. Tang, J. Fuh, Y. Wong, L. Lu, and H. Loh, "Micro-rapid-prototyping via multi-layered photo-lithography," *The International Journal of Advanced Manufacturing Technology*, vol. 29, no. 9-10, pp. 1026–1032, July 2006.

[14] L. M. Picco, L. Bozec, A. Ulcinas, D. J. Engledew, M. Antognozzi, M. A. Horton, and M. J. Miles, "Breaking the speed limit with atomic force microscopy," *Nanotechnology*, vol. 18, pp. 044 030–1–044 030–4, 2007.

[15] B. Bhikkaji, M. Ratnam, A. J. Fleming, and S. O. R. Moheimani, "High-performance control of piezoelectric tube scanners." *IEEE Trans. on Control Systems Technology*, vol. 5, no. 5, pp. 853–866, September 2007.

[16] B. Bhikkaji, M. Ratnam, and S. O. R. Moheimani, "PVPF control of piezoelectric tube scanners." *Sensors and Actuators: A. Physical*, vol. 135, no. 2, pp. 700–712, April 2007.

[17] A. J. Fleming and S. O. R. Moheimani, "Sensorless vibration suppression and scan compensation for piezoelectric tube nanopositioners," *IEEE Trans. on Control Systems Technology*, vol. 14, no. 1, pp. 33–44, January 2006.

[18] S. S. Aphale, A. J. Fleming, and S. O. R. Moheimani, "High speed nano-scale positioning using a piezoelectric tube actuator with active shunt control," *Micro and Nano Letters*, vol. 2(1), no. 1, pp. 9–12, 2007.

[19] H. R. Pota, S. O. R. Moheimani, and M. Smith, "Resonant controllers for smart structures," *Smart Materials and Structures*, vol. 11, no. 1, pp. 1–8, 2002.

[20] N. Kodera, H. Yamashita, and T. Ando, "Active damping of the scanner for high-speed atomic force microscopy," *Review of Scientific Instruments*, vol. 76, no. 5, pp. 1–5, 2005.

[21] S. Devasia, E. Eleftheriou, and S. O. R. Moheimani, "A survey of control issues in nanopositioning," *IEEE Trans. on Control Systems Technology*, vol. 15, no. 5, pp. 802–823, September 2007.

[22] S. S. Aphale, A. J. Fleming, and S. O. R. Moheimani, "Integral resonant control of collocated smart structures," *Smart Materials and Structures*, vol. 16, pp. 439–446, 2007.

[23] ——, "A second-order controller for resonance damping and tracking control of nanopositioning systems," *in Proc. of the International Conference on Adaptive Structures and Technologies, Ascona, Switzerland*, 2008.

[24] K. K. Leang and S. Devasia, "Feedback-linearized inverse feedforward for creep, hysteresis, and vibration compensation in afm piezoactuators," *IEEE Transactions on Control Systems Technology*, vol. 15, no. 5, pp. 927–935, September 2007.

[25] L. Y. Pao, J. A. Butterworth, and D. Y. Abramovitch, "Combined feedforward/feedback control of atomic force microscopes," in *Proc. American Control Conference*, New York, July 2007, pp. 3509–3515.

[26] S. Devasia, "Review of feedforward approaches for nano precision positioning in high speed SPM operation," in *Proc. IFAC World Congress*, Seoul, Korea, July 2008, pp. 9221–9229.

[27] ——, "Should model-based inverse inputs be used as feedforward under plant uncertainty?" *IEEE Transactions on Automatic Control*, vol. 47, no. 11, pp. 1865–1871, November 2002.

[28] A. J. Fleming and A. G. Wills, "Optimal periodic trajectories for band-limited systems," *IEEE Transactions on Control Systems Technology*, no. To Appear, 2008.